Inorg. Chem. **2007**, *46*, 9503–9508

In Situ Ligand Reactions under Hydrothermal Conditions Afford a Novel Zinc-Substituted Polyoxovanadate Dimer

Shou-Tian Zheng,[†] Ming-Hui Wang,[‡] and Guo-Yu Yang*,[†]

State Key Laboratory of Structural Chemistry, Fujian Institute of Research on the Structure of Matter, Chinese Academy of Sciences, Fuzhou, Fujian 350002, China, and the School of Chemistry and Molecular Engeering, Qingdao University of Science & Technology, Qingdao, Shandong 266042, China

Received March 24, 2007

A novel polyoxovanadate (POV), $[Zn(2,2'\text{-bpy})_3]_4[(ppz)\{\{Zn(tepa)\}_2ZnAs_8V_{13}O_{41}(H_2O)\}_2][As_8V_{14}O_{42}(0.5H_2O)]_2\cdot 4H_2O$ (**1**, 2,2′-bpy = 2,2′-bipyridine, ppz = piperazine, tepa = tetraethylenepentamine), has been hydrothermally synthesized and structurally characterized by elemental analysis, IR spectra, thermogravimetric analysis, magnetic measurement, and single-crystal X-ray diffraction analysis. Crystal data for **1**: orthorhombic, *Aba*2, $a = 28.3414(14)$ Å, $b = 27.9995(16)$ Å, $c = 41.5819(16)$ Å, $V = 32997(3)$ Å^3, $Z = 4$, $\rho = 2.264$ mg·cm^{-3}. X-ray structure analysis shows that the structure of **1** consists of one unique zinc-substituted POV dimer and two POV monomers. Interestingly, the formation of the zinc-substituted POV dimer involves two new in situ ligand reactions under hydrothermal conditions, the intermolecular and intramolecular deamination coupling reactions of dien. Magnetization measurement revealed the presence of antiferromagnetic interaction between V^{IV} ions in **1**.

Introduction

During the past decade, research in the rapidly growing polyoxometalate (POM) area has been focused on the design and synthesis of TM-substituted POMs (TM = transition metal) because of their highly tunable nature and noteworthy spectroscopic, magnetic, and catalytic properties.[1] Because lots of lacunary polyoxotungstate (POT) anions, such as monovacant (e.g., α-$PW_{11}O_{39}$ and α-$P_2W_{17}O_{61}$), divacant (γ-$SiW_{10}O_{36}$), and trivacant (e.g α-PW_9O_{34} and α-$P_2W_{15}O_{56}$), not only can be easily made in one- or two-step processes in high yield but also have well-defined metal-binding sites,[2] and they are useful precursors for making TM-substituted POTs. Thus, large numbers of novel TM-substituted POTs have been reported to date and constituted the largest subclass of the TM-substituted POM family.[3]

On the other hand, almost all of the research activities of the design and synthesis of novel polyoxovanadate (POV) materials focus on the combination of TM complexes (TMC) and POVs by self-assemblies, to produce TMC-supported or TMC-linked POVs. Typical examples include TMC-supported discrete (0D) $[\{\{Zn(en)_2\}_2As_6V_{15}O_{42}(H_2O)\}_2\{Zn(en)_2\}]\cdot 2Hen\cdot 3H_2O$ and $[Zn_2(enMe)_2(en)_3][\{Zn(enMe)_2\}As_6V_{15}O_{42}(H_2O)]\cdot 4H_2O$,[4] TMC-linked 1D $[Cu(enMe)_2]_3[V_{15}O_{36}Cl]\cdot 2.5H_2O$ and $[Co(en)_3][\{Co(en)_2\}_2As_6V_{15}O_{42}]\cdot 4H_2O$,[5] 2D

* To whom correspondence should be addressed. Email: ygy@fjirsm.ac.cn. Fax: +86-591-83710051.
† Chinese Academy of Sciences.
‡ Qingdao University of Science & Technology.

(1) Borrás-Almenar, J. J.; Coronado, E.; Müller, A.; Pope, M. T. *Polyoxometalate Molecular Science*; Kluwer: Dordrecht, The Netherlands, 2004.
(2) *Inorganic Syntheses*; A. P. Ginsbergh, Ed.; Wiley & Sons: New York, 1990; Vol. 27.
(3) (a) Howell, R. C.; Perez, F. G.; Jain, S.; Horrocks, W. D.; Rheingold, A. L.; Francesconi, L. C. *Angew. Chem., Int. Ed.* **2001**, *40*, 4031. (b) Hussain, F.; Bassil, B. S.; Bi, L.; Reicke, M.; Kortz, U. *Angew. Chem., Int. Ed.* **2004**, *43*, 3485. (c) Mal, S. S.; Kortz, U. *Angew. Chem., Int. Ed.* **2005**, *44*, 3777. (d) Kortz, U.; Nellutla, S.; Stowe, A. C.; Dalal, N. S.; Rauwald, U.; Danquah, W.; Ravot, D. *Inorg. Chem.* **2004**, *43*, 2308. (e) Bi, L.; Kortz, U. *Inorg. Chem.* **2004**, *43*, 7961. (f) Mialane, P.; Dolbecq, A.; Sécheresse, F. *Chem. Commun.* **2006**, 3477. (g) Belai, N.; Pope, M. T. *Chem. Commun.* **2005**, 5760. (h) Mialane, P.; Dolbecq, A.; Marrot, J.; Rivière, E.; Sécheresse, F. *Chem.—Eur. J.* **2005**, *11*, 1771. (i) Mialance, P.; Dolecq, A.; Marrot, J.; Rivière, E.; Sécheresse, F. *Angew. Chem., Int. Ed*, **2003**, *42*, 3523. (j) Reinoso, S.; Vitoria, P.; Felices, L. S.; Lezama, L.; Gutiérrez-Zorrilla, J. M. *Inorg. Chem.* **2006**, *45*, 108. (k) Nogueira, H. I. S.; Paz, F. A. A.; Teixeira, P. A. F.; Klinowski, J. *Chem. Commun*. **2006**, 2953. (l) Godin, B.; Chen, Y.-G.; Vaisserman, J.; Ruhlmann, L.; Verdaguer, M.; Gouzerh, P. *Angew. Chem., Int. Ed*. **2005**, *44*, 3072.
(4) (a) Zheng, S.-T.; Zhang, J.; Yang, G.-Y. *Chem. Lett.* **2003**, 810. (b) Zheng, S.-T.; Chen, Y.-M.; Zhang, J.; Yang, G.-Y. *Z. Anorg. Allg. Chem.* **2006**, *632*, 159.
(5) (a) DeBord, J. R. D.; Haushalter, R. C.; Meyer, L. M.; Rose, D. J.; Zapf, P. J.; Zubieta, J. *Inorg. Chim. Acta* **1997**, *256*, 165. (b) Bu, W. M.; Yang, G.-Y.; Ye, L., Xu, J.-Q. *Chem. Lett.* **2000**, 462. (c) Zheng, S.-T.; Zhang, J.; Xu, J.-Q.; Yang, G.-Y. *J. Solid State Chem.* **2005**, *178*, 3740.

10.1021/ic700562m CCC: $37.00 © 2007 American Chemical Society
Published on Web 10/04/2007

$[M_2(en)_5][\{M(en)_2\}_2V_{18}O_{42}(X)]\cdot 9\ H_2O$ (M = Zn/Cd, X = $H_2O/Cl^-/Br^-$) and $[Co(en)_2]_2[Sb_8V_{14}O_{42}(H_2O)]\cdot 6H_2O$,[6] and 3D $[M(H_2O)_4]_3[V_{18}O_{42}(XO_4)]\cdot 24\ H_2O$ (M = Fe/Co; X = V/S) and $[\{Cu(1,2\text{-pn})_2\}_7\{V_{16}O_{38}(H_2O)\}_2]\cdot 4H_2O$.[7] Compounds $[Cu_4V_{18}O_{42}(NO_3)(enMe)_8]\cdot 10\ H_2O$ and $[Cu_4V_{18}O_{42}(SO_4)(enMe)_8]\cdot 10H_2O$ are recent examples,[8] which exhibit two rare 3D structures constructed from well-defined $\{V_{18}O_{42}\}$ clusters linked by copper complexes.

Now, the construction of a new type of POV materials is one of interesting and challenging issues in POM synthetic chemistry. Compared with abundant TM-substituted POTs, TM-substituted POVs are quite rare because it is hard to obtain steady lacunary POV precursors. So, the design and synthesis of TM-substituted POVs remains a great challenge for synthetic chemists. Lately, we discovered that TM ions, such as Ni^{2+}, Zn^{2+}, or Cd^{2+}, can substitute one/two VO_5 pyramids of arsenic−vanadium clusters to form mono/di-TM-substituted POVs.[9] Because the TMs can further coordinate to appropriate organic ligands, these Ni/Zn/Cd-substituted POVs not only provide several rare examples of TM-substituted POVs, but also exhibit a new type of inorganic−organic hybrid POMs containing inorganic polyoxoanions decorated directly with amine. Furthermore, organically derived POMs based on inorganic polyoxoanions linked by organic species have drawn tremendous attention.[10] Therefore, the design and synthesis of novel POM hybrids containing TM-substituted POVs that are further bridged by amine is another significant and challenging topic.

Additionally, in situ ligand synthesis has provoked significant interest in coordination chemistry and organic chemistry for discovering new organic reactions and making uncommon complexes obtained very difficultly by routine synthetic methods.[11] So far, more than 10 types of in situ ligand reactions under hydro(solvo)thermal conditions have been found,[12] such as hydroxylation of aromatic rings,[12a] decarboxylation,[12b] C−C bond formation by reductive or oxidative coupling,[12c] and so on. These reactions represent promising new routes for constructing novel coordination architectures. Here, we report the first example of in situ deamination coupling reaction (DCR) of dien under hydrothermal conditions, affording a novel zinc-substituted POV,

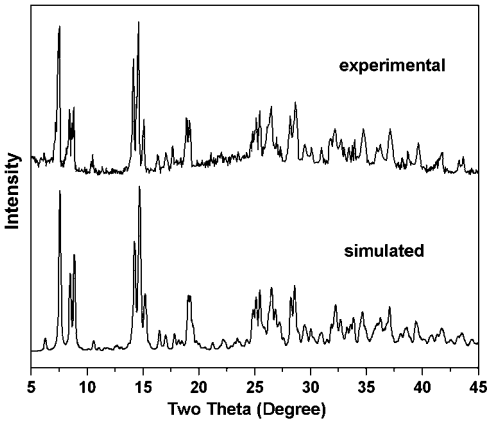

Figure 1. Simulated and experimental powder X-ray diffraction patterns of **1**.

$[Zn(2,2'\text{-bpy})_3]_4[(ppz)\{\{Zn(tepa)\}_2ZnAs_8V_{13}O_{41}(H_2O)\}_2]\text{-}[As_8V_{14}O_{42}(0.5H_2O)]_2\cdot 4H_2O$ (**1**).

Experimental Section

All of the chemicals employed in this study were analytical reagents. Elemental analyses of carbon, hydrogen, and nitrogen were carried out with a Vario EL III elemental analyzer. IR spectra (KBr pellets) were recorded on an ABB Bomen MB 102 spectrometer. Thermal analysis was performed in a dynamic oxygen atmosphere with a heating rate of 10 °C/min, using a METTLER TGA/SDTA851^e thermal analyzer. Variable-temperature susceptibility measurement was carried out in the temperature range 5−300 K at a magnetic field of 0.5 T for **1** on polycrystalline samples with a Quantum Design MPMS-5 magnetometer. The experimental susceptibilities were corrected for the Pascal's constants. An XRD spectrum was obtained using a Philips X'Pert-MPD diffractometer with Cu Kα radiation (λ = 1.54056 Å).

Synthesis of 1. Samples of V_2O_5(0.30 g) and As_2O_3(0.35 g) were stirred in 10 mL distilled water for 5 min, forming an orange mixed solution, and then a 0.60 mL (5.5 mmol) diethylenetriamine (dien) was added drop-by-drop with continuous stirring, turning the color to kelly green. Further, 0.80 g of $Zn(OAc)_2\cdot 4H_2O$ and 0.25 g of 2,2′-bpy are in turn added to this solution and stirred for 30 min. The resulting solution was sealed in a 35 mL stainless-steel reactor with a Teflon liner and heated at 160 °C for 3 days and was then cooled to room temperature (initial and final pH of 7.45 and 8.35, respectively). The solid product (0.268 g, 39.1% yield based on V_2O_5), consisting of single crystals in the form of a brown block, was recovered by filtration, washed with distilled water, and dried in air. Anal. Calcd (Found) for $C_{156}H_{206}As_{32}N_{46}O_{170}V_{54}Zn_{10}$ **1**: C, 16.64 (16.55); H, 1.85 (1.89); N, 5.73 (5.67). IR (KBr, cm^{-1}): 3455s, 1642s, 1608s, 1483m, 1449s, 1324m, 995s, 758s, 712s, 633m, 554m, 474m. Powder X-ray diffraction patterns of the bulk product **1** are in good agreement with the calculated patterns based on the results from single-crystal X-ray diffraction (Figure 1).

(6) (a) Khan, M. I.; Yohannes, E.; Doedens, R. J.; *Inorg. Chem*. **2003**, *42*, 3125. (b) Zhang, L.-J.; Zhao, X.-L.; Xu, J.-Q.; Wang, T.-G. *J. Chem. Soc., Dalton. Trans*. **2002**, 3275. (c) Zheng, S.-T.; Chen, Y.-M.; Zhang, J.; Xu, J.-Q.; Yang, G.-Y. *Eur. J. Inorg. Chem*. **2006**, 397.

(7) (a) Khan, M. I.; Yohannes, E.; Doedens, R. J. *Angew. Chem., Int. Ed*. **1999**, *38*, 1292. (b) Lin, B. Z.; Liu, S. X.; *Chem. Commun*. **2002**, 2126. (c) Liu, S. X.; Xie, L. H.; Gao, B.; Zhang, C. D.; Sun, C. Y.; Li, D. Hui, Su, Z. M. *Chem. Commun*. **2005**, 5023.

(8) Xu, Y.; Nie, L. B.; Zhu, D.; Song, Y.; Zhou, G. P.; You, W. S. *Cryst. Growth Des.* **2007**, *7* (5), 925.

(9) (a) Zheng, S.-T.; Zhang, J.; Yang, G.-Y. *Eur. J. Inorg. Chem*. **2004**, 2004. (b) Cui, X.-B.; Xu, J.-Q.; Meng, H.; Zheng, S.-T.; Yang, G.-Y. *Inorg. Chem*. **2004**, 43, 8005. (c) Zheng, S.-T.; Zhang, J.; Yang, G.-Y. *Inorg. Chem.* **2005**, *44*, 2426.

(10) (a) Gouzerh, P.; Proust, A. *Chem. Rev*. **1998**, *98*, 77. (b) Peng, Z. *Angew. Chem., Int. Ed*. **2004**, *43*, 930. (c) Mialance, P.; Duboc, C.; Marrot, J.; Rivière, E.; Dolbecq, A.; Sécheresse, F. *Chem.—Eur. J*. **2006**, *12*, 1950. (d) Atencio, R.; Briceño, A.; Silva, P.; Rodríguez, J. A.; Hanson, J. C. *New J. Chem*. **2007**, *31*, 33.

(11) (a) Kukushkin, V. Y.; Pombeiro, A. J. L. *Chem. Rev*. **2002**, *102*, 1771. (b) Zhang, X. *Coord. Chem. Rev*. **2005**, *249*, 1201. (c) Chen, X. M.; Tong, M. L. *Acc. Chem. Res.* **2007**, *40*, 162.

(12) (a) Zhang, J.; Lin, Y.; Huang, X.; Chen, X. *J. Am. Chem. Soc*. **2005**, *127*, 5495. (b) Su, C.; Goforth, A. M.; Smith, M. D.; Pellechia, P. J.; Loye, H. C. *J. Am. Chem. Soc*. **2004**, *126*, 3576. (c) Zheng, N.; Bu, X.; Feng, P. *J. Am. Chem. Soc*. **2002**, *124*, 9688. (d) Zhang, J.; Zheng, S.; Huang, X.; Chen, X. *Angew. Chem., Int. Ed*. **2004**, *43*, 206. (e) Lin, W.; Wang, Z.; Ma, L. *J. Am. Chem. Soc*. **1999**, *121*, 11249. (f) Xiong, R.; Zhang, J.; Chen, Z.; You, X.; Che, C.; Fun, K. *Dalton. Trans*. **2001**, 780. (g) Zhang, X.; Hou, J.; Wu, H. *Dalton. Trans*. **2004**, 3437. (h) Hu, X.; Xu, J.; Cheng, P.; Chen, X.; Cui, X.; Song, J.; Yang, G.; Wang, T. *Inorg. Chem*, **2004**, *43*, 2261. (i) Cheng, J.; Yao, Y.; Zhang, J.; Li, Z.; Cai, Z.; Zhang, X.; Cheng, Y.; Kang, Y.; Qin, Y.; Wen, Y. *J. Am. Chem. Soc*. **2004**, *126*, 7796.

Table 1. Crystallographic Data for **1** and **2**

compound	**1**	**2**
empirical formula	$C_{156}H_{206}As_{32}N_{46}O_{170}V_{54}Zn_{10}$	$C_{32}H_{118}As_{16}N_{24}O_{87}V_{24}Zn_8$
fw	11247.57	5175.74
cryst syst	orthorhombic	triclinic
space group	*Aba*2	$P\bar{1}$
a (Å)	28.3414(14)	15.5635(3)
b (Å)	27.9995(16)	19.6903(4)
c (Å)	41.5819(16)	24.8067(4)
α (deg)	90	85.215(5)
β (deg)	90	89.402(4)
γ (deg)	90	82.088(3)
V (Å^3)	32997(3)	7503(2)
Z	4	2
D_{calcd} (g cm^{-3})	2.264	2.291
μ (mm^{-1})	5.440	6.262
F(000	21 688	4988
θ range (deg)	$3.01 \le \theta \le 27.49$	$1.94 \le \theta \le 28.28$
limiting indices	$-36 \le h \le 33$, $-36 \le k \le 36$, $-49 \le l \le 54$	$-20 \le h \le 19$, $-23 \le k \le 26$, $-33 \le l \le 26$
GOF on F^2	1.035	1.055
R_1[a] [$I > 2\sigma(I)$]	0.0644	0.0893
wR_2[b] [$I > 2\sigma(I)$]	0.1575	0.2164

[a] $R_1 = \sum||F_o| - |F_c||/\sum|F_o|$. [b] $wR_2 = \{\sum[w(F_o^2 - F_c^2)^2/\sum[w(F_o^2)^2]]^{1/2}$; $w = 1/[\sigma^2(F_o^2) + (xP)^2 + yP]$, $P = (F_o^2 + 2F_c^2)/3$, where $x = 0.0961$ and $y = 287.4518$ for **1** and $x = 0.1205$ and $y = 21.9991$ for **2**.

Interestingly, a new compound $\{[Zn(dien)]_2(dien)_2[Zn_2As_8V_{12}O_{40}(0.5H_2O)]\}_2 \cdot 6H_2O$ (**2**) was obtained by using the same procedure as **1**, except that 0.80 g $Zn(OAc)_2 \cdot 4H_2O$ was first added to the orange $V_2O_5/As_2O_3/H_2O$ solution and stirred for 5 min before 0.60 mL dien was added dropwise (36.3% yield based on V_2O_5). Anal. Calcd (Found) for $C_{32}H_{118}As_{16}N_{24}O_{87}V_{24}Zn_8$ **2**: C, 7.42 (7.35); H, 2.30 (2.62); N, 6.49 (6.41). IR (KBr, cm^{-1}): 3440s, 2945w, 1623s, 1456m, 1343w, 984s, 722s, 639m, 543m, 460m (Figure S1 in the Supporting Information).

In addition, **1** also can be directly made by replacing dien with tepa and ppz. Details are as follows: samples of V_2O_5 (0.30 g) and As_2O_3 (0.35 g) were stirred in 10 mL distilled water for 5 min, and then a 0.84 mL (4.4 mmol) tepa was added drop-by-drop with continuous stirring, followed by 0.21 g (1.1 mmol) piperazine hexahydrate. Further, 0.80 g $Zn(OAc)_2 \cdot 4H_2O$ and 0.25 g 2,2′-bpy are in turn added to the solution and stirred for 30 min. Finally, the pH of this solution was adjusted from 7.55 to 8.35 by 25% ammonia solution. The resulting solution was sealed in a 35 mL stainless-steel reactor with a Teflon liner and heated at 160 °C for 3 days and was then cooled to room temperature (final pH 8.73). The brown solid product (0.453 g) was recovered by filtration, washed with distilled water, and dried in air. Both IR spectra and X-ray analysis confirmed that the solid product is **1**.

X-ray Analysis. Single crystals with dimensions of $0.45 \times 0.50 \times 0.85$ mm^3 and $0.20 \times 0.22 \times 0.25^3$ mm for **1** and **2**, respectively, were selected for single-crystal X-ray diffraction analysis. Data were collected on a Siemens SMART CCD diffractometer with graphite-monochromated Mo Kα radiation ($\lambda = 0.71073$ Å) at 293 K. All of the absorption corrections were performed with the *SADABS* program.[13] Both structures were solved by direct methods and refined by full-matrix least-squares methods on F^2 using the *SHELXTL97* program package.[14] In **1** and **2**, all of the non-hydrogen atoms except for a few isolated and disordered H_2O molecules were refined anisotropically. All of the hydrogen atoms of the organic ligands were geometrically placed and refined using a riding model. However, the hydrogen atoms of the water molecules have not been included in the final refinement. For **1**, a total of 112 698 reflections were collected with 33 482 unique ones ($R_{int} = 0.0584$), of which 29 402 reflections with $I > 2\sigma(I)$ were used for structural elucidation. At convergence, $R_1(wR_2)$ was 0.0644 (0.1575) and the goodness-of-fit was 1.035. The final Fourier map had a minimum and maximum of −2.691 and 2.563 e·Å^{-3}. For **2**, a total of 60 745 reflections were collected with 35 832 unique ones ($R_{int} = 0.0463$), of which 23 357 reflections with $I > 2\sigma(I)$ were used for structural elucidation. At convergence, $R_1(wR_2)$ was 0.0893 (0.2164) and the goodness-of-fit was 1.055. The final Fourier map had a minimum and maximum of −2.178 and 2.170 e·Å^{-3}. Unusually, a few crystallographically independent atoms including 8 arsenic, 4 vanadium, and 16 oxygen atoms in **2** are disordered, and each of them occupies two sites with a refined occupancy of 0.5 for each site. A detailed description of the disordered model can be seen in the Supporting Information. Crystallographic data of **1** and **2** are summarized in Table 1. CCDC numbers of 266152 and 650738 exist for **1** and **2**, respectively.

Results and Discussion

Brown crystals of **1** were obtained by hydrothermal reaction of V_2O_5, As_2O_3, dien, $Zn(OAc)_2 \cdot 4H_2O$, and 2,2′-bpy in water. One interesting feature is that the dien molecules as a starting amine transform not only to ppz via in situ intramolecular DCR (Scheme 1.1) but also to tepa via in situ intermolecular DCR (Scheme 1.2) in the formation of **1**. Both tepa and ppz are captured by zinc ions to form mononuclear $[Zn(tepa)]^{2+}$ and binuclear $[Zn_2(ppz)]^{4+}$ complexes, which are further incorporated into the backbone of the POV dimer in **1**. To our knowledge, such a kind of in situ ligand reaction has never been observed before. In addition, attempts were made to obtain **1** using tepa and ppz as starting materials instead of dien. The reaction works under

(13) Sheldrick, G. M. *SADABS, Program for Siemens Area Detector Absorption Corrections*; University of Göttingen: Göttingen, Germany, 1997.

(14) a) Sheldrick, G. M. *SHELXS97, Program for Crystal Structure Solution*; University of Göttingen: Göttingen, Germany, 1997. (b) Sheldrick, G. M. *SHELXL97, Program for Crystal Structue Refinement*; University of Göttingen: Göttingen, Germany, 1997.

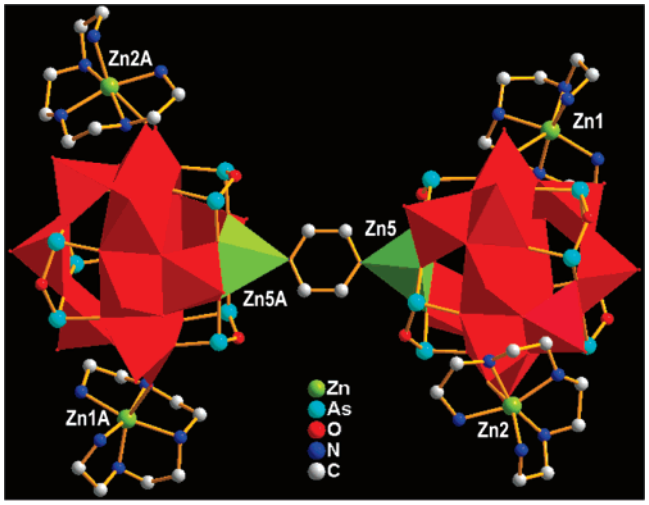

Figure 2. View of the structure of **1a**.

Scheme 1. In situ Deaminizing Coupling Reactions of Dien Molecules

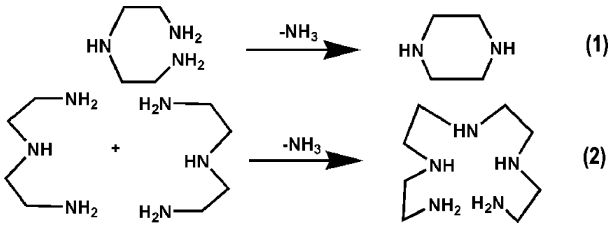

established starting pH and molar ratios of tepa and ppz (Synthesis Section).

X-ray analyses revealed that the molecular structure of **1** consists of one neutral zinc-substituted POV dimer [(ppz)-{{Zn(tepa)}$_2$ZnAs$_8$V$_{13}$O$_{41}$(H$_2$O)}$_2$] (**1a**) and two well-known POV monomers[15] [As$_8$V$_{14}$O$_{42}$(0.5H$_2$O)]$^{4-}$, as well as four isolated [Zn(2,2′-bpy)$_3$]$^{2+}$ complexes acting as charge compensation (part a of Figure S2 in the Supporting Information). The unique structure of **1a** can be described as follows. First, the mono-zinc-substituted [ZnAs$_8$V$_{13}$O$_{40}$(H$_2$O)]$^{4-}$ unit in **1a** can be derived from anion [As$_8$V$_{14}$O$_{42}$(0.5H$_2$O)]$^{4-}$ by replacing one of the two [V═O]$^{2+}$ groups located between As$_2$O$_5$ groups with one Zn^{2+} ion (parts b and c of Figure S2 in the Supporting Information). It is notable that no mono-zinc-substituted POV has been reported to date. Second, as shown in Figure 2, the [ZnAs$_8$V$_{13}$O$_{40}$(H$_2$O)]$^{4-}$ unit acts as a ligand and coordinates to two [Zn(tepa)]$^{2+}$ groups to generate a neutral bi-TMC-supported [Zn(tepa)$_2$ZnAs$_8$V$_{13}$O$_{41}$(H$_2$O)] unit. Finally, two such neutral units are further linked together by ppz ligands via Zn−N bonds, resulting in the formation of the first amine-bridged POV dimer.

It is noteworthy that the coexistence of a neutral POV dimeric hybrid and the inorganic POV anion in **1** is a unique feature in the POV chemistry.[16] In addition, **1** consists of three types of complexes, [Zn(2,2′-bpy)$_3$]$^{2+}$, [Zn(tepa)]$^{2+}$, and [Zn$_2$(ppz)]$^{4+}$. The zinc sites in these complexes display two

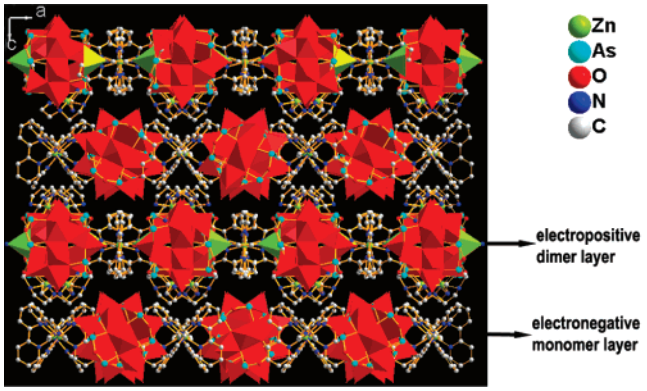

Figure 3. View of the 3D structure of **1** along the *b* axis.

different coordination environments, distorted octahedra (Zn1/Zn2/Zn3/Zn4 and their symmetry equivalent atoms) and square pyramids (Zn5 and its symmetry equivalent atom). Each octahedral geometry around Zn1/Zn1A/Zn2 /Zn2A is defined by five nitrogen atoms from one tepa ligand (Zn−N 1.963(11)−2.244(10) Å) and one terminal oxygen atom of one pyramidal vanadium site in the cluster (Zn−O 2.344-(1)−2.574(1) Å), whereas each octahedral geometry around Zn3/Zn3A/Zn4/ Zn4A is defined by six nitrogen atoms from three 2,2′-bpy (Zn−N 2.111(10)−2.175(9) Å). Each square-pyramidal geometry around Zn5/Zn5A is formed by four basal μ_3-oxo groups from the cluster shell and one apical nitrogen atom from the ppz ligand (Zn5−O 2.022(8)−2.050-(7) Å, Zn5−N 2.046(9) Å). Finally, the 3D structure of **1** is constructed from alternatively stacking electropositive dimer layers and electronegative monomer layers along the *c* axis (Figures 3 and S3 in the Supporting Information).

In **1**, all of the As−O distances are in the range of 1.703-(12)−1.837(11) Å, and all the vanadium centers have a distorted VO$_5$ square-pyramidal environment with V−O bond distances in the usual range of 1.532(9)−1.628(8) and 1.871-(10)−2.042 (9) Å for terminal oxygen and μ_3-O atoms, respectively. Bond-valence sum calculations[17] show the oxidation states of all of the vanadium and arsenic atoms are +4 and +3, respectively, which are consistent with the overall charge balance of formula **1**.

Interestingly, the same starting materials as **1** but with different sampling sequences lead to a new **2** without involving in situ DCRs of dien (Experimental Section). As shown in Figure 4, compared with **1a**, the molecular structure of **2** is also a dimer but constructed from two crystallographically independent bi-zinc-substituted anions [Zn$_2$As$_8$V$_{12}$O$_{40}$(0.5H$_2$O)]$^{4-}$ (**2a**). First, the **2a** unit can be derived from anion [As$_8$V$_{14}$O$_{42}$(0.5H$_2$O)]$^{4-}$ by replacing both [V═O]$^{2+}$ groups located between As$_2$O$_5$ groups with two Zn^{2+} ions. Second, two **2a** units are respectively linked to two [Zn(dien)]$^{2+}$ complexes by bridging dien ligands via Zn−N bonds (Zn−N 1.978(9)−2.320(3) Å), resulting in the formation of two neutral {[Zn(dien)]$_2$(dien)$_2$[Zn$_2$As$_8$V$_{12}$O$_{42}$-(0.5H$_2$O)]} units, which are further joined together through a weak Zn6−O bond (2.876(2) Å) to form dimeric structure

(15) Huan, G. H.; Greaney, M. A.; Jacobson, A. J. *J. Chem. Soc., Chem. Commun.* **1991**, 261.
(16) Mialane, P.; Dolbecq, A.; Lisnard, L.; Mallard, A.; Marrot, J.; Sécheresse, F. *Angew. Chem., Int. Ed.* **2002**, 2398.
(17) Brown, I. D.; Altermatt, D. *Acta Crystallogr., Sect. B* **1985**, *41*, 244.

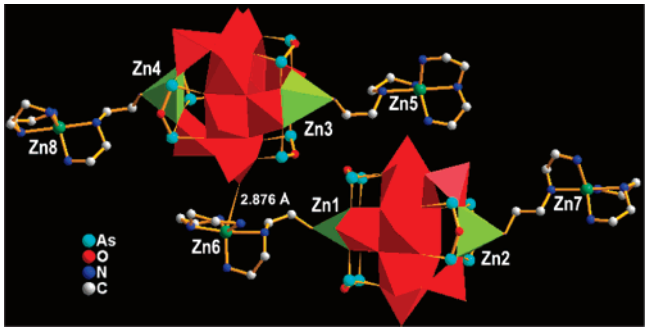

Figure 4. View of the molecular structure of **2**.

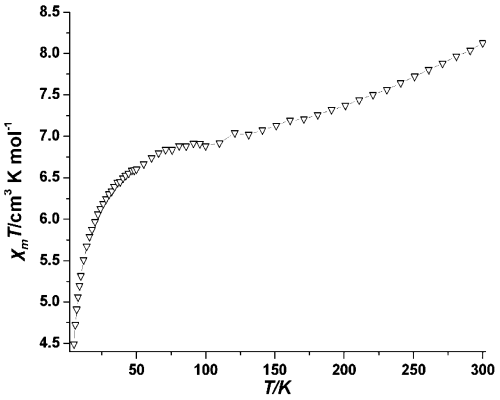

Figure 5. Temperature dependences of the product $\chi_M T$ for **1**.

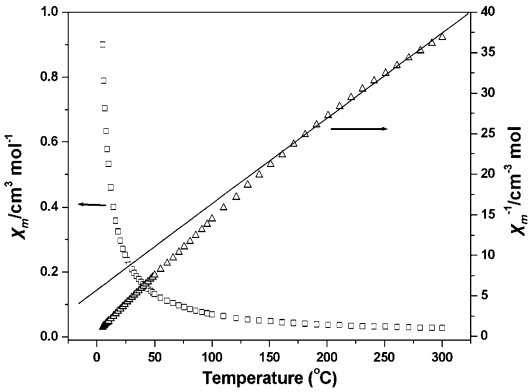

Figure 6. Temperature dependence of χ_m (□) and χ_m^{-1}(Δ) for **1**.

2. In **2**, all of the V═O, V−O, and As−O bond lengths fall in the ranges 1.583(16)−1.627(8), 1.905(9)−2.032(15), and 1.711(13)−1.823(14) Å, respectively. Bond-valence sum calculations show the oxidation states of all of the vanadium and arsenic atoms are +4 and +3, respectively, which are consistent with the overall charge balance of formula **2**. It is notable that one **2a** unit in **2** is normal, whereas another **2a** unit contains a few disordered vanadium, arsenic, and oxygen atoms, which have been refined as two sets of atoms. The detailed description of the disordered models can be seen in the Supporting Information (Figure S4).

The variable-temperature magnetic susceptibility of **1** was measured between 5 and 300 K (Figures 5 and 6). The $\chi_M T$ value of **1** at 300 K is 8.13 cm^3 Kmol^{-1} (8.06 μ_B), much smaller than that expected for the total spin-only value 20.25

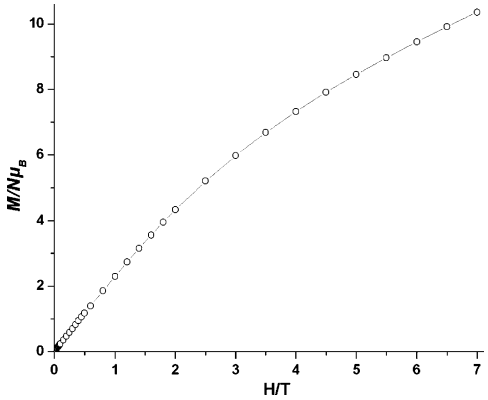

Figure 7. Magnetization measurement, in the reduced form of $M/N\ \mu_B$, in the field range 0−7 T at 2 K of **1**.

cm^3 Kmol^{-1} (12.73 μ_B) of 54 noninteracting V^{4+} ions with $S = {}^1/_2$ and $g = 2$. As the temperature decreases, the $\chi_M T$ value decreases to 105 K to stabilize approximately at 6.90 cm^3 Kmol^{-1}, and then starts to decrease again, reaching 4.50 cm^3 Kmol^{-1} (6.0 μ_B) at 5.0 K. The temperature dependences of $\chi_M T$ for **1** demonstrate the existence of strong antiferromagnetic coupling interaction, which is a common feature for most POV culsters.[18] The temperature dependence of the reciprocal susceptibilities (χ_m^{-1}) lacks linear relationship over a wide temperature range, the fit to the Curie−Weiss law above 150 K gives a value of $\theta = -55.0$ K, which supports the presence of strong antiferromagnetic coupling between the V^{4+} ions. The isothermal magnetization $M(H)$ at 2 K with a field of up to 70 kOe has been represented in Figure 7. The magnetization increases almost linearly from 0 to 70 kOe and reaches 10.40 $N\beta$ at 70 kOe, far from the saturation value $MS = 54\ N\beta$ for 54 V^{4+} ions ($S = {}^1/_2$). This behavior strongly indicates the antiferromagnetic coupling between V^{4+} ions. Because no suitable theoretical model is available in the literature for such a complex system,[19] further studies on the magnetic properties are in progress.

Conclusions

In summary, we have made the first dimeric zinc-substituted POV. This study not only further demonstrates that some vanadium sites of arsenic−vanadium POMs can be substituted by bivalent TMs but also introduces the amine linker into an extremely unusual combination with POV framework, which may open up possibilities for making a new type of TM-substituted inorganic−organic hybrid POVs. Such complexes may induce new chemical and physical properties. Furthermore, the work also discovered two new in situ ligand reactions under hydrothermal conditions and intermolecular and intramolecular deaminizing coupling reactions of dien. This kind of in situ reaction not only

(18) (a) Müller, A.; Peters, F.; Pope, M. T.; Gatteschi, D. *Chem. Rev.* **1998**, *98*, 239. (b) Müller, A.; Sessoli, R.; Krickemeyer, E.; Bögge, H.; Meyer, J.; Gatteschi, D.; Pardi, L.; Westphal, J.; Hovemeier, K.; Rohlfing, R.; Döring, J.; Hellweg, F.; Beugholt, C.; Schmidtmann, M. *Inorg. Chem.* **1997**, *36*, 5239.
(19) Kahn, O. *Molecular Magnetism*; VCH: New York, 1993.

enriches the study of in situ ligand synthesis under hydro-(solvo)thermal conditions, but also represents a promising new route for constructing novel complexes.

Acknowledgment. This work was supported by the National Natural Science Fund for Distinguished Young Scholar of China (20725101), 973 Program (Grant 2006CB-932904), the NNSF of China (Grant 20473093), the NSF of Fujian Province (Grant E0510030), and the Key Project from CAS (Grant KJCX2.YW.H01).

Supporting Information Available: Crystal data in CIF format, IR spectra, TG plot, additional experimental details, and structural figures. This material is available free of charge via the Internet at http://pubs.acs.org.

IC700562M